Tunneling Spectroscopy of M_3C_{60} Superconductors: The Energy Gap, Strong Coupling, and Superconductivity

ZHE ZHANG, CHIA-CHUN CHEN, CHARLES M. LIEBER*

Tunneling spectroscopy has been used to characterize the magnitude and temperature dependence of the superconducting energy gap (Δ) for K_3C_{60} and Rb_3C_{60}. At low temperature the reduced energy gap, $2\Delta/kT_c$ (where T_c is the transition temperature) has a value of 5.3 ± 0.2 and 5.2 ± 0.3 for K_3C_{60} and Rb_3C_{60}, respectively. The magnitude of the reduced gap for these materials is significantly larger than the value of 3.53 predicted by Bardeen-Cooper-Schrieffer theory. Hence, these results show that the pair-coupling interaction is strong in the M_3C_{60} superconductors. In addition, measurements of Δ(*T*) for both K_3C_{60} and Rb_3C_{60} exhibit a similar mean-field temperature dependence. The characterization of Δ and Δ(*T*) for K_3C_{60} and Rb_3C_{60} provides essential constraints for theories evolving to describe superconductivity in the M_3C_{60} materials.

SUPERCONDUCTIVITY IN ALKALI METAL–doped buckminsterfullerene is now well established (*1–10*), although the mechanism remains an open and intensely investigated question. To date, experimental studies have elucidated several important properties of the superconducting phase, including the face-centered cubic (fcc) structure (*5, 6*), the coherence length (*7*), and the penetration depth (*7, 8*). Investigations of the dependence of the transition temperature (T_c) on the fcc lattice constant (*6*) and on pressure (*9, 10*) have further led to the interesting proposal that changes in T_c can be explained through variations in the density of electronic states (DOS) at the Fermi level (E_f). Specifically, using the expression $T_c \propto \hbar\omega\exp(-1/NV)$ from BCS (Bardeen-Cooper-Schrieffer) theory, where $\hbar\omega$ is the excitation energy relevant to electron pairing, N is the DOS at E_f, and V is the electron-phonon coupling strength, it has been suggested that variations in N determine observed changes in T_c, while V and $\hbar\omega$ are essentially constant (*2, 6, 9*).

Implicit in this analysis is the assumption of weak coupling. Theoretical and experimental studies have also argued, however, that the coupling interaction might be strong (*11–13*), and hence we have sought to define unambiguously the relative strength of the coupling in the M_3C_{60} superconductors. The superconducting energy gap (Δ) provides a measure of the coupling strength and can therefore address this issue. In particular, weak-coupling BCS theory predicts that there is a universal value for the reduced energy gap, $2\Delta/kT_c$, of 3.53 (*14*). We have recently reported a preliminary value for the reduced energy gap of Rb_3C_{60} that is significantly larger than this weak-coupling limit (*11*); however, it is not known whether this large value of the reduced energy gap is universal for the M_3C_{60} superconductors or how Δ depends on temperature. Herein, we describe detailed tunneling spectroscopy studies of the superconducting energy gap of single phase K_3C_{60} and Rb_3C_{60} that answer these questions.

Tunneling spectroscopy is a particularly attractive technique to probe the energy gap since the conductance (*dI/dV*) determined from current-voltage (*I-V*) data provides a direct measure of the DOS (*15*). Because the M_3C_{60} superconductors have short coherence lengths (*7*), conventional planar junctions prepared on sintered pellets could show extrinsically broadened energy gap features (that is, owing to nonuniform tunneling barriers), and thus we have used a low-temperature scanning tunneling microscope (STM) to make point junctions with a sharpened metal tip. Our data show that the reduced energy gap in the M_3C_{60} materials is independent of M and significantly larger than the weak coupling limit of 3.5. In addition, Δ(*T*) exhibits a mean field temperature dependence with the energy gap disappearing at the bulk value of T_c. The implications of these new results to the mechanism of superconductivity in the M_3C_{60} materials are discussed.

Single-phase K_3C_{60} and Rb_3C_{60} materials were prepared by reaction of alkali-metal alloy or alkali-metal with C_{60} as described in detail elsewhere (*3, 4*). Briefly, a 3:1 mixture of MHg or M (M = K, Rb) and C_{60} were sealed under vacuum in a quartz tube and then heated at 200°C. When the shielding fraction of M_3C_{60} superconducting phase reached about 40%, the tube was opened and the polycrystalline powder was pressed into 3-mm-diameter pellets. The pellets were sintered at 200°C until the shielding fraction approached 100%. Magnetization versus temperature curves typical of the K_3C_{60} and Rb_3C_{60} samples used in this study are shown in Fig. 1. The transition temperatures of these K- and Rb-doped materials are 19 and 29 K, respectively, and the low temperature shielding fractions are approximately 100% for both samples.

Magnetically characterized M_3C_{60} sintered pellets were mounted on the STM sample holder using silver paint in an inert atmosphere glove box ($[O_2] \approx [H_2O] \approx 1$ ppm). The sample holder was then transferred to the STM which is contained within a vacuum can. The sample is exposed to the atmosphere for a few minutes during the transfer process; however, its superconducting properties do not degrade significantly. After mounting the sample, the evacuated STM assembly was placed in a mechanically and acoustically isolated helium dewar. The metal (tip)-insulator-superconductor (N-I-S) junction was made by mechanically stepping the tip to the sample and then adjusting the junction resistance and position using the tube scanner of the STM. Tunneling measurements were made either through vacuum when the sample surfaces were metallic ($T > T_c$) or in point contact. In the latter case we believe that the partially oxidized sample surface functions as the insulating barrier. The data obtained from these two distinct types of junctions were similar. *I-V* curves were recorded digitally using custom-built electronics under computer control; the sample temperature was actively maintained for temperatures greater than 4.2 K. Several independent samples of K_3C_{60} and Rb_3C_{60} were examined in these studies, and typically at least 30 *I-V* curves were recorded at each temperature for each independent sample; the reported data are

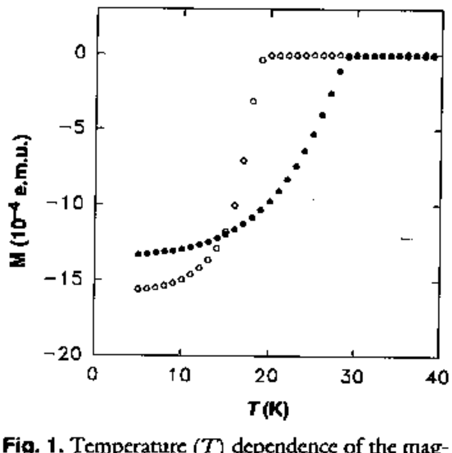

Fig. 1. Temperature (*T*) dependence of the magnetization obtained for a 4.1-mg K_3C_{60} sintered pellet (open circles) and a 3.8-mg Rb_3C_{60} sintered pellet (filled circles). The T_c's of the K_3C_{60} and Rb_3C_{60} samples are 19.0 and 28.6 K, respectively. The curves were recorded by cooling in zero field to 5 K and subsequent warming in a 10-Oe field. The shielding fractions estimated from these curves are approximately 100%.

Department of Chemistry and Division of Applied Sciences, Harvard University, Cambridge, MA 02138.

*To whom correspondence should be addressed.

representative of this extensive data set.

A series of I-V curves recorded at temperatures of 20, 10, and 4.2 K on a K_3C_{60} sample are shown in Fig. 2, A to C, respectively. The curve recorded at 4.2 K exhibits features characteristic of the superconducting energy gap, including (i) a distinct zero-current regime about E_f (V = 0), and (ii) conductance onsets at $V \approx \pm 4$ mV. We believe that this structure, which is observed in most of the I-V curves recorded at 4.2 K, reflects the modulation in I due to the gap (2Δ) in the DOS of K_3C_{60} probed in the N-I-S tunneling geometry. Similar features are also observed in I-V curves recorded on Rb_3C_{60} samples at 4.2 K (Fig. 2D), although the conductance onsets, $V \approx \pm 6$ mV, occur at distinctly larger bias voltage.

Other possible explanations for this structure in the I-V curves are a coulomb blockade or superconductor-insulator-superconductor (S-I-S) tunneling. We believe, however, that both of these possibilities are unlikely. First, we do not find that $I \propto V^2$ for small V as predicted and previously observed for Coulomb charging (*16, 17*). Furthermore, we find that the magnitude of the zero current region around V = O is reproducible, in K_3C_{60} and systematically larger in Rb_3C_{60} (Fig. 2, C and D), and that for both materials the gap-like structure disappears for $T > T_c$; neither of these observations is consistent with the coulomb blockade. Secondly, for S-I-S tunneling there should be a sharp current jump at $V = 2\Delta$ (*15*), and not the smooth increase observed in our data. In addition, it is unlikely that the same S-I-S tunneling would be observed for vacuum and point contact tunneling, and thus we believe that the conductance onsets can be assigned with confidence to $\pm\Delta$. Lastly, we note that a small number of I-V curves recorded at 4.2 K exhibit large gaps which may be interpreted as S-I-S tunneling; conditions for reproducible observation of this large gap structure are not yet known, and thus we believe it is premature to interpret such data.

An important point evident upon examination of the 4.2 K I-V curves is that the gap structure for K_3C_{60} is significantly smaller than for Rb_3C_{60}. These results indicate qualitatively that Δ scales with T_c. To quantitatively assess the magnitude of Δ and the reduced energy gap we have calculated the normalized conductance, $(dI/dV)_S/(dI/dV)_N$ where the subscripts N and S refer to the normal and superconducting states (Fig. 3). Since $(dI/dV)_S/(dI/dV)_N$ is proportional to the superconducting DOS, N_S, the value of Δ can be determined from a fit of normalized conductance to a model for the DOS. We find that good fits of the experimental data are obtained using the broadened BCS function proposed by Dynes and co-workers, $N_S = \mathrm{Re}[|E-i\Gamma|/((E-i\Gamma)^2-\Delta^2)^{1/2}]$, where E is the energy of the tunneling electron and Γ is a broadening function (*18*). Dynes *et al.* introduced Γ specifically to account for shortened quasiparticle lifetime, however, here we use Γ as a phenomenological parameter since the mechanism of broadening is not known (for example, it could be due to inelastic scattering or strong coupling effects). The essential result obtained from the fits to the 4.2 K K_3C_{60} data is that the experimental value of Δ, 4.4 meV, is significantly larger than the $T \rightarrow 0$ BCS theory prediction of 2.73 meV. Furthermore, the average value of Δ (4.2 K) determined from these experiments yields a reduced energy gap, $2\Delta/kT_c \pm 1$ SD, of 5.3 ± 0.2 for K_3C_{60}. The value of the reduced energy gap at 4.2 K for Rb_3C_{60} reported recently (*11*) and further refined in this study, 5.2 ± 0.3, is the same within experimental error, and thus Δ clearly scales with T_c in these materials. The large value of $2\Delta/kT_c$ for the M_3C_{60} superconductors shows that the coupling in these materials is strong. Although we are unaware of other experimental studies confirming strong coupling, two recent theoretical calculations have predicted that the coupling in K_3C_{60} will be strong (*12, 13*).

It is interesting to consider the implications of strong coupling. Within the context of phonon-mediated pairing, theoretical work has shown that large values of Δ arise

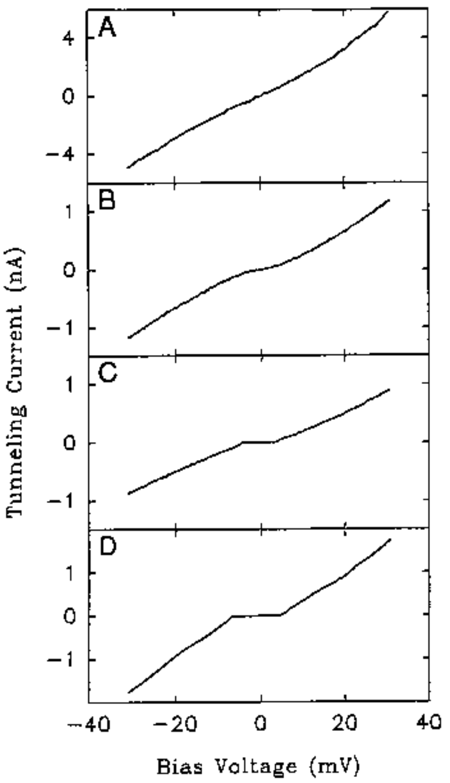

Fig. 2. Current versus voltage (I-V) curves recorded on a K_3C_{60} sample at (**A**) 20 K, (**B**) 10 K, and (**C**) 4.2 K, and on a Rb_3C_{60} sample at 4.2 K (**D**). Typically, five sequential I-V measurements at a specific sample location were averaged to produce a single curve; these data were not subject to other smoothing routines.

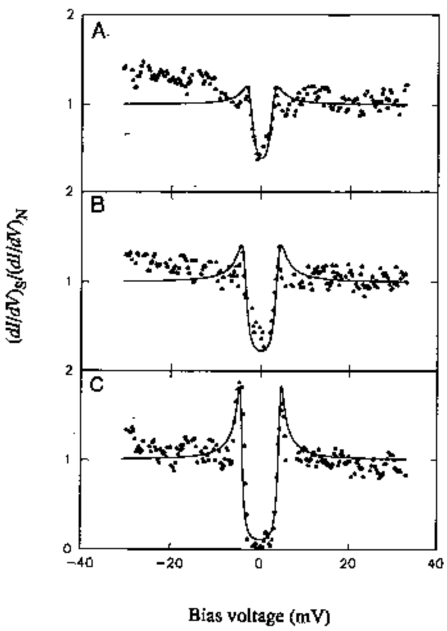

Fig. 3. Normalized conductance versus voltage $[(dI/dV)_S/(dI/dV)_N]$ curves for K_3C_{60} corresponding to temperatures of (**A**) 15 K, (**B**) 10 K, and (**C**) 4.2 K. The experimental data (filled circles) were obtained by numerically differentiating the I-V data and then normalizing by dI/dV at 20 K. The solid lines correspond to the best fits of this data to the expression $(dI/dV)_S/(dI/dV)_N = \mathrm{Re}[|E - i\Gamma|/((E - i\Gamma)^2 - \Delta^2)^{1/2}]$. The values of the energy gap Δ and broadening function Γ in meV are (A) $\Delta = 3.0$; $\Gamma = 1.1$, (B) $\Delta = 4.0$; $\Gamma = 0.9$, (C) $\Delta = 4.4$; $\Gamma = 0.5$.

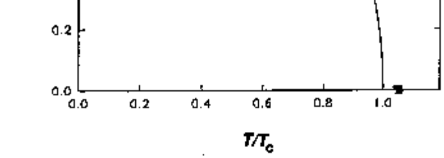

Fig. 4. Summary of the temperature-dependent energy gap results for K_3C_{60} (■) and Rb_3C_{60} (▽). For comparison the values of Δ have been normalized by the respective low temperature (4.2 K) values and the temperature has been scaled by T_c. The solid line corresponds to the temperature dependence of $\Delta(T)/\Delta(0)$ predicted by BCS theory (*14*).

from strong coupling to low frequency modes (*19*). In the M_3C_{60} materials, the most obvious low frequency modes are C_{60}-C_{60} intermolecular vibrations or C_{60} rotations. Alternatively, it has been suggested that the M^+ optical phonon could lead to strong coupling (*13*). High-frequency intramolecular C_{60} modes, which have been implicated in weak-coupling analyses (*2, 6*), are unlikely to yield the large value of $2\Delta/kT_c$ determined experimentally. Although additional work is needed to define whether the electron-phonon interaction is the operative coupling mechanism and if so, the mode relevant to pairing, our finding of strong coupling should be accounted for in models of superconductivity in these materials.

We have also characterized the temperature dependence of Δ in both K_3C_{60} and Rb_3C_{60} since this can provide additional insight into the mechanism of superconductivity. Representative normalized conductance curves recorded on K_3C_{60} and theoretical fits to these data for $4.2\ K < T < T_c$ are shown in Fig. 3. Qualitatively, we find that Δ decreases as T approaches T_c, and disappears for $T > T_c$. We have summarized the results from these temperature-dependent studies of Δ for K_3C_{60} and for Rb_3C_{60} by plotting $\Delta(T)/\Delta(4.2)$ versus T/T_c (Fig. 4). This figure explicitly shows that the normalized energy gaps of Rb_3C_{60} and K_3C_{60} exhibit a similar temperature dependence, and furthermore, that these data follow the universal temperature dependence predicted by BCS theory. Importantly, our $\Delta(T)$ data indicate that it may be possible to explain superconductivity using a mean-field theory (like BCS) modified for strong coupling. It is also interesting to consider real-space models of superconductivity since the coherence lengths in these materials are so short ($\xi \approx 25$ Å). In particular, it has been suggested that a Bose-Einstein condensation of real-space pairs may explain superconductivity in the short coherence length ($\xi_{ab} \approx 10$ Å) high-T_c copper oxide materials (*20, 21*). Since $\Delta(T)$ should exhibit a relatively sharp transition near T_c in a Bose-Einstein condensation, we believe that the observed temperature dependence of Δ argues against this interesting possibility.

In conclusion, tunneling spectroscopy has been used to define the energy gap in the M_3C_{60} superconductors. These experimental results have shown that (i) the pair coupling in these materials is strong, (ii) the energy gap scales with T_c, and (iii) the energy gap exhibits a universal temperature dependence. Regardless of the mechanism of pairing in the M_3C_{60} system, we believe that our results will be important constraints for any theoretical explanation of superconductivity in these materials.

REFERENCES AND NOTES

1. A. F. Hebard *et al.*, *Nature* **350**, 600 (1991).
2. M. J. Rosseinsky *et al.*, *Phys. Rev. Lett.* **66**, 2830 (1991).
3. K. Holczer *et al.*, *Science* **252**, 1154 (1991).
4. C.-C. Chen, S. P. Kelty, C. M. Lieber, *ibid.* **253**, 886 (1991).
5. P. W. Stephens *et al.*, *Nature* **351**, 632 (1991).
6. R. M. Fleming *et al.*, *ibid.* **352**, 787 (1991).
7. K. Holczer *et al.*, *Phys. Rev. Lett.* **67**, 271 (1991).
8. Y. J. Uemura *et al.*, *Nature* **352**, 605 (1991).
9. G. Sparn *et al.*, *Science* **252**, 1829 (1991).
10. J. E. Schirber *et al.*, *Physica C* **178**, 137 (1991).
11. Z. Zhang, C. C. Chen, S. P. Kelty, H. Dai, C. M. Lieber, *Nature* **353**, 333 (1991).
12. S. C. Erwin and W. E. Pickett, *Science*, in press.
13. F. C. Zhang, M. Ogata, T. M. Rice, *Phys. Rev. Lett.*, in press.
14. J. Bardeen, L. N. Cooper, J. R. Schrieffer, *Phys. Rev.* **108**, 1175 (1957).
15. E. L. Wolf, *Principles of Tunneling Spectroscopy* (Oxford University Press, New York, 1989).
16. D. V. Averin and K. K. Likharev, *J. Low Temp. Phys.* **62**, 345 (1986).
17. P. J. M. van Bentum, H. van Kempen, L. E. C. van de Leemput, P. A. A. Teunissen, *Phys. Rev. Lett.* **60**, 369 (1988); R. Berthe and J. Halbritter, *Phys. Rev. B* **43**, 6880 (1991).
18. R. C. Dynes, V. Narayanamurti, J. P. Garno, *Phys. Rev. Lett.* **41**, 1509 (1978).
19. B. Mitrović, C. R. Leavens, J. P. Carbotte, *Phys. Rev. B* **21**, 5048 (1980).
20. R. Friedberg and T. D. Lee, *ibid.* **40**, 6745 (1989).
21. Z. Schlesinger *et al.*, *ibid.* **41**, 11237 (1990); B. N. J. Persson and J. E. Demuth, *ibid.* **42**, 8057 (1990).

22. We thank Z. Schlesinger and J. E. Demuth of IBM for helpful discussions. Supported by the David and Lucile Packard, Alfred P. Sloan, Camille and Henry Dreyfus, and National Science Foundations (C.M.L.).

13 October 1991; accepted 1 November 1991

Eighth Millennium Pottery from a Prehistoric Shell Midden in the Brazilian Amazon

A. C. Roosevelt, R. A. Housley, M. Imazio da Silveira, S. Maranca, R. Johnson

The earliest pottery yet found in the Western Hemisphere has been excavated from a prehistoric shell midden near Santarém in the lower Amazon, Brazil. Calibrated accelerator radiocarbon dates on charcoal, shell, and pottery and a thermoluminescence date on pottery from the site fall from about 8000 to 7000 years before the present. The early fishing village is part of a long prehistoric trajectory that contradicts theories that resource poverty limited cultural evolution in the tropics.

Amazonia has been described as sparsely occupied by small Indian groups in prehistoric times. The resource poverty of the tropical forest habitat was thought to have precluded permanent settlement, population growth, and cultural development. Complex cultures with pottery and agriculture were supposed to have spread from the Andes and Mesoamerica and decayed in the unfavorable tropical environment (*1–4*). Archeological evidence, however, reveals a sequence that is changing understanding of the ecology of cultural evolution in the Americas. An important new finding is that the age of pottery now appears to have begun earlier in Amazonia than elsewhere in the hemisphere.

Although stereotyped as resource-poor (*5*), Amazonia has large areas of alluvial soils (*6*) that would not have presented severe limitations to human adaptation. In fact, researchers working between 1830 and 1945 uncovered evidence for cultural development: deep stratified middens, earthworks, elaborate art and artifacts, and abundant ancient biological remains (*7–11*). Later, archeologists dismissed this research as not scientific and focused on excavating pottery, assuming most other material was not preserved; they took contemporary foragers and shifting horticulturalists as models for prehistory and interpreted complex cultures as ephemeral foreign invasions (*2–4*). This view was criticized on environmental and archeological grounds (*12–14*), but it persisted in the empirical vacuum and

A. C. Roosevelt, Department of Anthropology, Field Museum of Natural History, Chicago, 60605–2496.
R. A. Housley, Radiocarbon Accelerator Unit, Oxford University, Oxford, OX1 3QJ, England.
M. Imazio da Silveira, Arqueologia, Museu Paraense Emilio Goeldi, CP 399, 66.000, Belem, PA, Brazil.
S. Maranca, Museu de Arqueologia e Etnologia, Universidade de São Paulo, São Paulo, SP 42.503, Brazil.
R. Johnson, Zoology, Museum of Comparative Zoology, Harvard University, Cambridge, MA 02138.

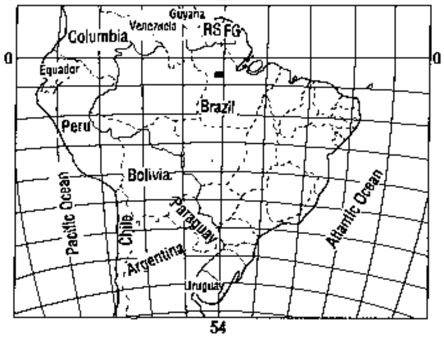

Fig. 1. Location of Santarém in Brazil.